Inorganic Chemistry

Article

pubs.acs.org/IC

Anion-Induced Supramolecular Isomerism in Two Preyssler P_5W_{30} Polyoxometalate-Based Hybrid Materials

Ya-Qin Zhao,[†] Kai Yu,[‡] Li-Wei Wang,[†] Ying Wang,[†] Xing-Po Wang,[†] and Di Sun*[,†]

[†]Key Lab of Colloid and Interface Chemistry, Ministry of Education, School of Chemistry and Chemical Engineering, Shandong University, Jinan, 250100, People's Republic of China

[‡]School of Chemistry and Chemical Engineering, Harbin Normal University, Harbin 150025, People's Republic of China

Supporting Information

ABSTRACT: Two extended Preyssler P_5W_{30} polyoxometalate-based inorganic−organic hybrid materials exhibiting anion-induced supramolecular isomerism were reported. Because of the *cis*−*trans* isomerism in the octahedral CoN_2O_4 coordination geometry, the Preyssler P_5W_{30} polyoxometalates are extended by double O−Co−O bridges in **1*α*** and a single O−Co−O bridge in **1*β*** to form the isomeric 2D 4-connected 4^4-**sql** and 3D 8-connected **bcu** networks, respectively. Both compounds show electrocatalytic abilities on the reduction of H_2O_2.

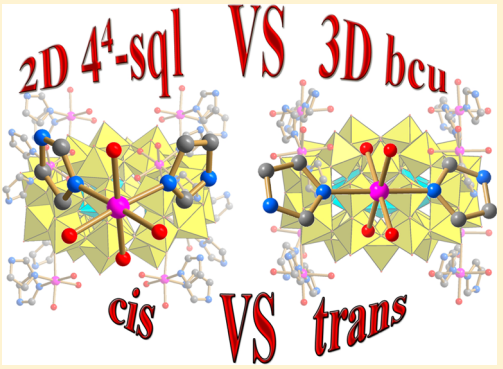

INTRODUCTION

Polyoxometalates (POMs) are eye-catching inorganic secondary building blocks (ISBBs) for constructing diverse hybrid materials. They do not merely supply substantial basic O atoms as polydentate inorganic linkers, but show various chemical compositions, dimensions, and geometric shapes as well as rich physical and chemical properties.[1] In this field, incorporation of 3d transition metal ions to decorate POMs could change their topological structures and properties. However, compared to much work on the decoration of small POMs (the number of W or Mo in one cluster < 20) to extended networks,[2] larger POMs, such as the Preyssler POM,[3] $\{P_5W_{30}\}$, which comprises five PW_6 subunits and totally 90 O atoms covered on the shell (30 μ_1-O and 60 μ_2-O), are less investigated as ISBBs. Although it has many superiorities, including (i) high acid or base stability over a wide pH range of 1−10; (ii) more surface oxygen atoms and high negative charges to bind more transition metal ions; and (iii) its internal cavity with a diameter of about 5 Å can accommodate distinct cations with proper diameters,[4] until now, only sporadic examples including some discrete metal-centered Preyssler clusters and extended Preyssler clusters by external decoration have appeared in literature.[5] With these regards, to create infinite Preyssler POMs-related hybrid frameworks appeared to be a fairly difficult task.

On the other hand, supramolecular isomerism[6] is an appealing phenomenon in supramolecular and coordination chemistry.[7−14] With the ever-increasing appearance of publications about supramolecular isomerism, supramolecular isomerism in polymeric network structures becomes not too surprising; however, supramolecular isomerism was hard to be observed in POM-based hybrid materials.[15]

Herein, we first report on a pair of anion-induced supramolecular isomers incorporating the *cis*−*trans* isomerism of the octahedral coordination geometry around the Co(II) center (Scheme 1), which is responsible for the resultant

Scheme 1. *Cis* and *Trans* Isomerism of Octahedral CoN_2O_4 Coordination Geometry in 1*α* and 1*β*

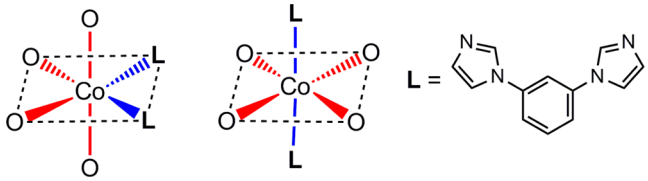

isomeric 2D 4-connected 4^4-**sql** and 3D 8-connected **bcu** networks with the formulas of $\{Co_4(dimb)_4(H_2O)_8[K(H_2O)H_6P_5W_{30}O_{110}]\}_n$ (**1*α***·122H_2O and **1*β***·90H_2O; dimb = 1,3-di(1*H*-imidazol-1-yl)benzene), respectively.

EXPERIMENTAL SECTION

Materials and General Methods. All chemicals and solvents used in the syntheses were of analytical grade and used without further purification. IR spectra were recorded on a Nicolet AVATAT FT-IR360 spectrometer as KBr pellets in the frequency range of 4000−400 cm^{-1}. The elemental analyses (C, H, N contents) were determined on a Vario EL III analyzer. Elemental analyses of K, P, W, and Co were performed by a Leaman inductively coupled plasma

Received: July 1, 2014
Published: October 1, 2014

   dx.doi.org/10.1021/ic501567s | *Inorg. Chem.* 2014, 53, 11046−11050

Table 1. Crystal Data for 1α and 1β

	1α	1β
empirical formula	$C_{48}H_{40}Co_4KN_{16}O_{119}P_5W_{30}$	$C_{48}H_{40}Co_4KN_{16}O_{119}P_5W_{30}$
formula weight	8690.13	8690.13
temperature (K)	180(2)	298(2)
crystal system	orthorhombic	orthorhombic
space group	*Fmmm*	*Immm*
a (Å)	18.1962(17)	18.9064(12)
b (Å)	28.429(3)	20.9843(13)
c (Å)	34.905(3)	23.4284(16)
volume (Å^3)	18056(3)	9294.9(10)
Z	4	2
ρ_{calc} (mg/mm^3)	3.197	3.105
μ (mm^{-1})	19.537	18.976
F(000)	15256.0	7628.0
2Θ range for data collection	3.7−50°	4.3−50°
reflections collected	22624	23277
independent reflections	4273 [*R*(int) = 0.0732]	4455 [*R*(int) = 0.0514]
data/parameters	4273/338	4455/408
goodness-of-fit on F^2	1.069	1.043
final *R* indexes [$I \geq 2\sigma(I)$]	R_1 = 0.0650, wR_2 = 0.1586	R_1 = 0.0468, wR_2 = 0.1335
final *R* indexes [all data]	R_1 = 0.0858, wR_2 = 0.1660	R_1 = 0.0618, wR_2 = 0.1436

(ICP) spectrometer. Powder X-ray diffraction (PXRD) data were collected on a Philips X'Pert Pro MPD X-ray diffractometer with Cu Kα radiation equipped with an X'Celerator detector. Thermogravimetric analyses (TGA) were performed on a Netzsch STA 449C thermal analyzer from room temperature to 800 °C under a nitrogen atmosphere at a heating rate of 10 °C/min. Electron paramagnetic resonance (EPR) spectra of solid samples were recorded on a Bruker X-band EPR spectrometer equipped with a temperature controller. Electrochemical measurements were performed with a CHI660 electrochemical workstation. A conventional three-electrode system was used. The working electrode was a modified carbon paste electrode (CPE). A Ag/AgCl (3 M KCl) electrode was used as a reference electrode and a Pt wire as a counter electrode.

Synthesis of Complex 1α. A mixture of $K_{12.5}Na_{1.5}[NaP_5W_{30}O_{110}]\cdot 15H_2O$ (82.4 mg, 0.01 mmol), 1,3-di(1*H*-imidazol-1-yl)benzene (10.5 mg, 0.05 mmol), and $Co(NO_3)_2\cdot 6H_2O$ (43.7 mg, 0.15 mmol) was dissolved in 6 mL of H_2O and stirred for 10 min at room temperature. The resulting mixture was sealed in a 25 mL Teflon-lined stainless steel autoclave and heated at 160 °C for 3000 min, after which, it was cooled over 13 h to room temperature. The product was obtained as pink rodlike crystals in 40% yield (based on cobalt). Anal. Calcd. (found) for $C_{48}H_{284}Co_4KN_{16}O_{241}P_5W_{30}$: C, 5.30 (5.68); H, 2.63 (2.58); N, 2.06 (2.30); P, 1.42 (1.85); K, 0.36 (0.22); Co, 2.17 (2.86); W, 50.66 (50.24) %.

Synthesis of Complex 1β. The synthesis of **1β** was similar to that of **1α**, but using $CoCl_2\cdot 6H_2O$ (35.7 mg, 0.15 mmol) instead of $Co(NO_3)_2\cdot 6H_2O$. The product was obtained as mixed pink rodlike (**1α**) and yellow block-shaped crystals (**1β**), which are separated manually, giving **1β** in 25% yield (based on cobalt). Anal. Calcd. (found) for $C_{48}H_{220}Co_4KN_{16}O_{209}P_5W_{30}$: C, 5.59 (5.55); H, 2.15 (2.87); N, 2.17 (2.01); P, 1.50 (1.96); K, 0.38 (0.26); Co, 2.29 (2.75); W, 53.49 (53.12) %

RESULTS AND DISCUSSION

Structure Descriptions of 1α and 1β. **1α** and **1β** are found to crystallize in face- and body-centered orthorhombic lattices with space groups of *Fmmm* and *Immm*, respectively, by X-ray single-crystal crystallographic analysis (Table 1). There are one-eighth of $[K(H_2O)H_6P_5W_{30}O_{110}]^{8-}$ and a half of a $[Co(dimb)(H_2O)_2]^{2+}$ unit in their asymmetric units. The valences of W (+6) and Co (+2) atoms were verified by bond valence sum (BVS) calculations.[16] The Preyssler-type P_5W_{30} POM is the same in **1α** and **1β**, and five PO_4^{3-} ions in the interior support the tire-like W_{30} shell. The 5-fold passes through the central axis of the W_{30} tire, giving it a perfect 5-fold symmetry. Five P atoms are in a mirror plane perpendicular to the central axis. Among 30 W atoms, 20 are distributed on the two treads and the remaining 10 are on the two sidewalls of the tire: each of the sidewall and tread contains 5 and 10 W atoms, respectively. All W centers are coordinated by six O atoms, forming the WO_6 octahedron. The bond distances between W and O in **1α** and **1β** are 1.67(4)−1.79(3) and 1.702(14)−1.74(2) Å for μ_1-O atoms, 1.80(3)−2.011(13) and 1.850(12)−2.036(9) Å for μ_2-O atoms, and 2.209(14)−2.308(18) and 2.21(2)−2.264(12) Å for μ_3-O atoms, respectively, which are comparable to the related compounds.[17] The Na ion is not presented in the central cavity of **1α** and **1β**, but replaced by K ion, which is a common phenomenon and also proved by the inductively coupled plasma (ICP) spectrometer. The outer Co(II) center is surrounded by four O atoms, two from POM and the other two from aqua, and two imidazole N atoms, giving an octahedral geometry. As illustrated in Figure 1a,b, eight Co(II) centers (four "above" and four "below") in total are anchored onto each P_5W_{30} POM via eight terminal oxygen atoms distributed in two inner W_{10} planes in two isomers. Although the P_5W_{30} anion has up to 30 terminal O atoms accessible to form coordination bonds with metal centers, not all of them could bind metal centers due to electronic and steric hindrance effects.

The most different structural feature in **1α** and **1β** is the *cis*−*trans* isomeric octahedral coordination geometry around the Co(II) center, as represented in Figure 1c,d. The broad electron paramagnetic resonance (EPR) spectra (Figure S1, Supporting Information) feature from 20 to 380 mT unambiguously indicates the presence of the high spin Co(II) ($S = 3/2$, d^7) at 40 K, and the differences in EPR also confirm the dissimilar coordinated atom arrangement around the Co(II) centers in **1α** and **1β**, which ultimately caused the Preyssler P_5W_{30} POMs in **1α** and **1β** to be extended to form isomeric 2D and 3D networks, respectively. For **1α**, each Preyssler P_5W_{30} POM is linked to its one neighbor (totally four

dx.doi.org/10.1021/ic501567s | *Inorg. Chem.* 2014, 53, 11046−11050

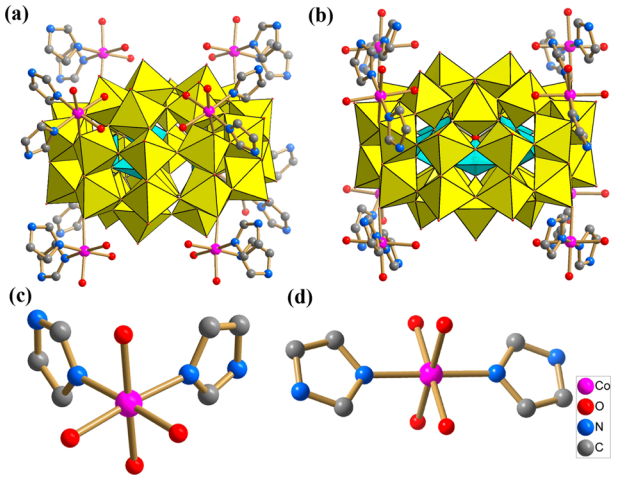

Figure 1. Views of molecular structures and coordination details of cobalt(II) centers in **1*α*** (a) and **1*β*** (b). The *cis* (c) and *trans* (d) octahedral coordination geometry around the Co(II) center in **1*α*** and **1*β***.

neighbors) through double O−Co−O bridges (Figure 2a,b), so it becomes a 4-connected node, despite that each P_5W_{30} links

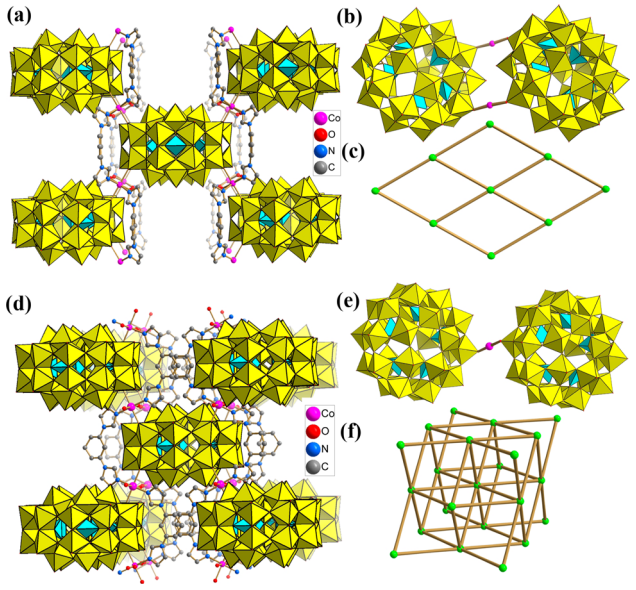

Figure 2. (a) P_5W_{30} POM linked to its four neighbors through four double O−Co−O bridges in **1*α***. (b) The linkage mode between two adjacent P_5W_{30} POMs in **1*α***. (c) The simplified 2D 4^4-**sql** network of **1*α***. (d) P_5W_{30} POM linked to its eight neighbors through eight single O−Co−O bridges in **1*β***. (e) The linkage mode between two adjacent P_5W_{30} POMs in **1*β***. (f) The simplified 3D 8-connected **bcu** network of **1*β***.

eight Co(II) centers. As a result, the 2D 4-connected 4^4-**sql** network (Figure 2c) along the *ab* plane formed in **1*α***. Differently, in **1*β***, each Preyssler P_5W_{30} POM is linked to its one neighbor (totally eight neighbors) through a single O−Co−O bridge (Figure 2d,e), and so it retains an 8-connected node. As a result, the 3D 8-connected **bcu** network (Figure 2f) formed in **1*β***. In fact, each dimb as a bidentate ligand clamps a pair of Co(II) centers anchored on the same one P_5W_{30} POM in **1*α*** and **1*β***, so it contributes nothing to the extension of the P_5W_{30}-based networks. However, due to *cis* or *trans* arrangement of the dimb ligand around the Co(II) centers, steric requirements dictate the linkage between adjacent P_5W_{30} POMs through a double or single O−Co−O bridge, thus determining the resultant networks.

Induced Effect of the Anions. The **1*α*** was obtained as a single phase using $Co(NO_3)_2{\cdot}6H_2O$, whereas concomitant crystallization of **1*α*** and **1*β*** occurred when using $CoCl_2{\cdot}6H_2O$, so it would be of interest to see if the predominant formation of **1*β*** could be induced by adding much more Cl^- ions. When different amounts of NaCl were deliberately added during synthesis of **1*α***, both **1*α*** and **1*β*** still appeared in the final products, but the quality percentage of **1*β*** increased with the amount of NaCl in the range of 0.1−2.0 mmol. Further increasing the amount of NaCl could not give a higher yield of **1*β*** (max. 87%). (Figure 3). These results clearly showed the

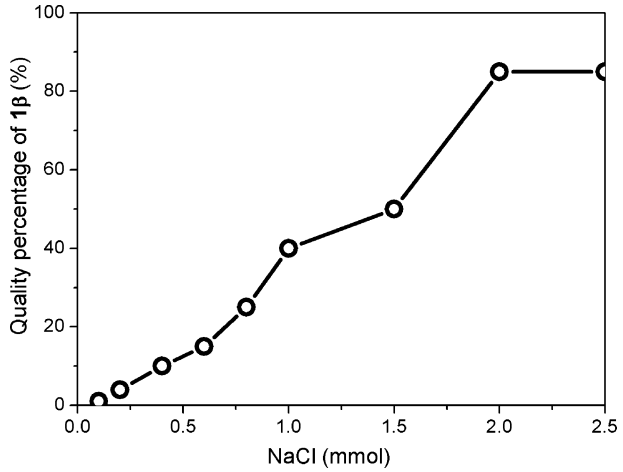

Figure 3. Plot of quality percentage of **1*β*** vs amount of NaCl.

obvious induced effect of the Cl^- anion on the formation of supramolecular isomer, **1*β***. Although both NO_3^- and Cl^- did not participate in the resultant networks, they exerted different bonding abilities and orientations toward the Co(II) ion at the beginning of the self-assembly in the solutions, which may affect the subsequent bonding directions of the organic linker and Preyssler P_5W_{30} POMs, causing the occurrence of the supramolecular isomerism in this system.

Voltammetric Behavior of 1*α*- and 1*β*-CPEs. The electrochemical behaviors of **1*α*** and **1*β*** were studied in 1 mol/L sulfuric acid aqueous solution at changing scanning speed. As depicted in Figure 4a,b, from −1.0 to 1.0 V, three pairs of reversible peaks related to oxidation−reduction reactions are detected for **1*α***- and **1*β***-CPE. The average peak potentials $E_{1/2} = 0.5(E_{pa} + E_{pc})$ of I/I′, II/II′, and III/III′ are −0.56, −0.12, and +0.51 V for **1*α***-CPE as well as −0.54, −0.29, and +0.47 V, for **1*β***-CPE (on account of the cyclic voltammogram at 100 mV s^{-1} shown in Figure S2, Supporting Information). Two pairs of redox peaks, II/II′ and III/III′, for **1*α***- and **1*β***-CPE are attributed to two successive double electron processes of the modified $\{P_5W_{30}\}$ polyoxoanion.[18] Redox peaks I−I′ in the positive directions for **1*α***- and **1*β***-CPE should be ascribed to the redox couple of Co^{III}/Co^{II}.[19] The differences in the peak positions between the parent $\{P_5W_{30}\}$ and **1*α*** and **1*β*** are attributed to the incorporation of the Co(II) ions, whereas the different coordination environments around Co(II) in **1*α*** and **1*β*** cause their different redox performance. The cathodic peaks of **1*α*** and **1*β*** move to the lower potentials,

dx.doi.org/10.1021/ic501567s | *Inorg. Chem.* 2014, 53, 11046−11050

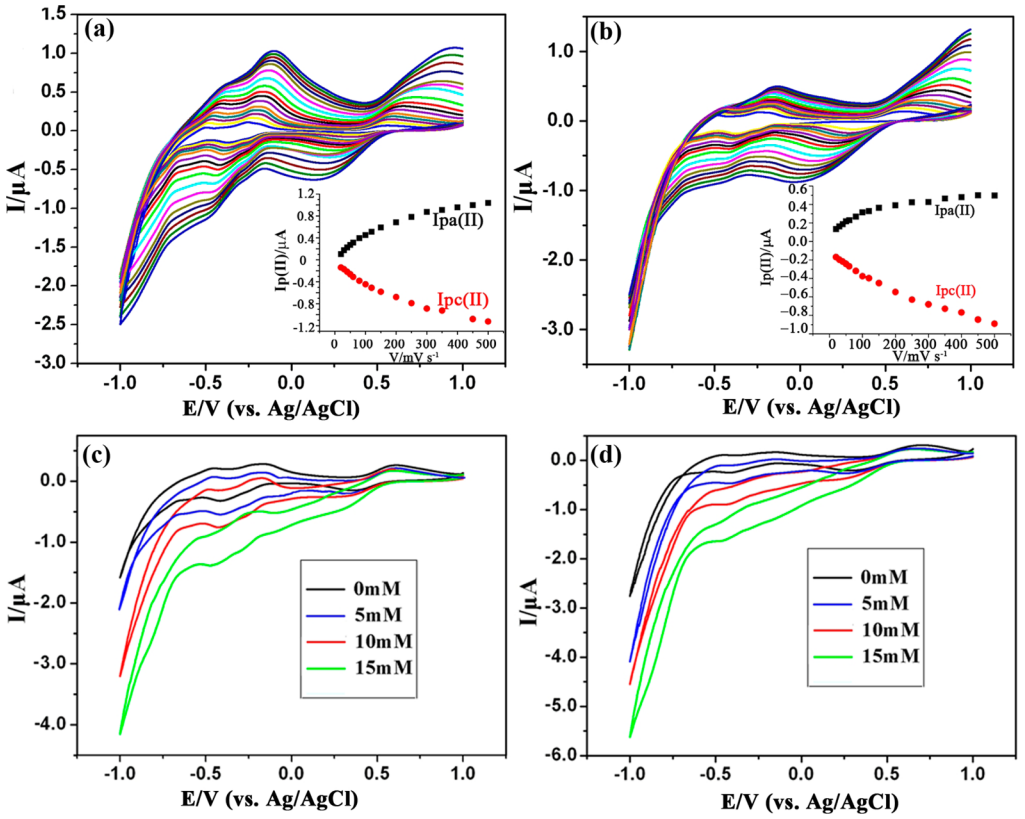

Figure 4. (a, b) Cyclic voltammograms of the **1*α***- and **1*β***-CPEs in 1 mol/L sulfuric acid aqueous solution at different scanning speeds (from inside to outside: 20, 30, 40, 50, 60, 80, 100, 120, 150, 200, 250, 300, 350, 400, 450, 500 mV s^{-1}). Inset: The plotting of peak current (II) of anode and cathode versus scanning speed. (c, d) Cyclic voltammograms of the **1*α***- and **1*β***-CPEs in 1 mol/L sulfuric acid aqueous solution containing 0.0, 5.0, 10.0, and 15.0 mmol/L H_2O_2 with a scanning speed of 40 mV/s.

whereas the corresponding anodic peaks move to the higher potentials when enhancing scanning speed, as depicted in Figure 4. When the scanning speed increased from 20 to 500 mV s^{-1}, the peak potentials also vary progressively. Furthermore, although the increase of the separation between the paired oxidative and reductive peaks was clearly discriminated, the mean peak potentials are basically maintained as a whole. The plotting of peak current (II) of anode and cathode versus scanning speed (see inset plots in Figure 4a,b) suggests that the redox processes of **1*α***- and **1*β***-CPE that occurred on the surface are populated when the scanning speed is lower than 100 mV s^{-1}, whereas, at a scanning speed higher than 100 mV s^{-1}, the peak currents were proportional to the square root of the scanning speed, indicating the diffusion-controlled redox processes.[20] It is also of note that **1*α***- and **1*β***-CPE are highly stable. When the range of potential is sustained between −1.0 and 1.0 V, the peak currents remain almost unaffected over 300 cycles at a scanning speed of 100 mV s^{-1}.

Electrocatalytic Activity of 1*α*- and 1*β*-CPEs for the Reduction of H_2O_2. Furthermore, **1*α***- and **1*β***-CPE show electrocatalytic abilities on the reduction of H_2O_2 (Figure 4c,d). At the **1*α***- and **1*β***-CPE, with the increase of the concentration of H_2O_2 from 0.0 to 15.0 mmol/L, increase of reduction peak currents and at the same time, the decrease of the corresponding oxidation peak currents were observed, indicating that H_2O_2 was reduced by two species of P_5W_{30} polyoxoanion.[20] For comparison, the electroreduction of H_2O_2 at a naked electrode usually needs a high overpotential and no noticeable response could be detected at a bare CPE. The results demonstrate that **1*α***- and **1*β***-CPEs have electrocatalytic abilities on the reduction of H_2O_2.

CONCLUSIONS

In conclusion, **1*α*** and **1*β*** represent the first examples of supramolecular isomeric Preyssler P_5W_{30}-based inorganic−organic hybrids depended on different anions. The supramolecular isomerism originated from the *cis*−*trans* octahedral CoN_2O_4 coordination geometry, which causes isomeric 2D 4-connected 4^4-**sql** and 3D 8-connected **bcu** networks to be obtained. Both compounds show electrocatalytic abilities on the reduction of H_2O_2.

ASSOCIATED CONTENT

Supporting Information

Synthesis procedure, tables, crystal data in CIF files, EPR, IR, CV, TGA, and powder X-ray diffractogram for **1*α*** and **1*β*** (CCDC 1008983−1008984). This material is available free of charge via the Internet at http://pubs.acs.org.

AUTHOR INFORMATION

Corresponding Author

*E-mail: dsun@sdu.edu.cn (D.S.).

Notes

The authors declare no competing financial interest.

■ ACKNOWLEDGMENTS

This work was supported by the NSFC (Grant No. 21201110), China Postdoctoral Science Foundation funded project (2013T60663).

■ REFERENCES

(1) (a) Izarova, N. V.; Pope, M. T.; Kortz, U. *Angew. Chem., Int. Ed.* **2012**, *51*, 9492−9510. (b) Müller, A.; Pope, M. T.; Todea, A. M.; Bogge, H.; van Slageren, J.; Dressel, M.; Gouzerh, P.; Thouvenot, R.; Tsukerblat, B.; Bell, A. *Angew. Chem., Int. Ed.* **2007**, *46*, 4477−4480. (c) Mitchell, S. G.; Streb, C.; Miras, H. N.; Boyd, T.; Long, D. L.; Cronin, L. *Nat. Chem.* **2010**, *2*, 308−312. (d) Miras, H. N.; Cooper, G. J. T.; Long, D. L.; Bogge, H.; Müller, A.; Streb, C.; Cronin, L. *Science* **2010**, *327*, 72−74. (e) Coronado, E.; Gomez−Garcia, C. J. *Chem. Rev.* **1998**, *98*, 273−296. (f) Sadakane, M.; Steckhan, E. *Chem. Rev.* **1998**, *98*, 219−238. (g) Proust, A.; Matt, B.; Villanneau, R.; Guillemot, G.; Gouzerh, P.; Izzet, G. *Chem. Soc. Rev.* **2012**, *41*, 7605−7622.

(2) (a) Wee, L. H.; Wiktor, C.; Turner, S.; Vanderlinden, W.; Janssens, N.; Bajpe, S. R.; Houthoofd, K.; Van Tendeloo, G.; De Feyter, S.; Kirschhock, C. E. A.; Martens, J. A. *J. Am. Chem. Soc.* **2012**, *134*, 10911−10919. (b) Nogueira, H. I. S.; Paz, F. A. A.; Teixeira, P. A. F.; Klinowski, J. *Chem. Commun.* **2006**, 2953−2955. (c) Li, Y. G.; Dai, L. M.; Wang, Y. H.; Wang, X. L.; Wang, E. B.; Su, Z. M.; Xu, L. *Chem. Commun.* **2007**, 2593−2595. (d) Bi, Y. F.; Du, S. C.; Liao, W. P. *Chem. Commun.* **2011**, *47*, 4724−4726. (e) Ishii, Y.; Takenaka, Y.; Konishi, K. *Angew. Chem., Int. Ed.* **2004**, *43*, 2702−2705. (f) Bakri, R.; Booth, A.; Harle, G.; Middleton, P. S.; Wills, C.; Clegg, W.; Harrington, R. W.; Errington, R. J. *Chem. Commun.* **2012**, *48*, 2779−2781.

(3) (a) Creaser, I.; Heckel, M. C.; Neitz, R. J.; Pope, M. T. *Inorg. Chem.* **1993**, *32*, 1573−1578. (b) Li, Y. Y.; Zhao, J. W.; Wei, Q.; Yang, B. F.; He, H.; Yang, G. Y. *Chem.—Asian. J.* **2014**, *9*, 858−867. (c) Zhang, Z. M.; Yao, S.; Li, Y. G.; Han, X. B.; Su, Z. M.; Wang, Z. S.; Wang, E. B. *Chem.—Eur. J.* **2012**, *18*, 9184−9188. (d) Wang, X. L.; Li, J.; Tian, A. X.; Lin, H. Y.; Liu, G. C.; Hu, H. L. *Inorg. Chem. Commun.* **2011**, *14*, 103−106. (e) Alizadeh, M. H.; Harmalker, S. P.; Jeannin, Y.; Martin-Frere, J.; Pope, M. T. *J. Am. Chem. Soc.* **1985**, *107*, 2662−2669. (f) Zhang, Z. M.; Yao, S.; Qi, Y. F.; Li, Y. G.; Wang, Y. H.; Wang, E. B. *Dalton. Trans.* **2008**, 3051−3053.

(4) (a) Fernandez, J. A.; Lopez, X.; Bo, C.; de Graaf, C.; Baerends, E. J.; Poblet, J. M. *J. Am. Chem. Soc.* **2007**, *129*, 12244−12253. (b) Kim, K. C.; Pope, M. T.; Gama, G. J.; Dickman, M. H. *J. Am. Chem. Soc.* **1999**, *121*, 11164−11170.

(5) (a) Qin, C.; Song, X. Z.; Su, S. Q.; Dang, S.; Feng, J.; Song, S. Y.; Hao, Z. M.; Zhang, H. J. *Dalton. Trans.* **2012**, *41*, 2399−2407. (b) Huang, L.; Cheng, L.; Wang, S. S.; Fang, W. H.; Yang, G. Y. *Eur. J. Inorg. Chem.* **2013**, 1639−1643. (c) Hussain, F.; Kortz, U.; Keita, B.; Nadjo, L.; Pope, M. T. *Inorg. Chem.* **2006**, *45*, 761−766.

(6) Hennigar, T. L.; Macquarrie, D. C.; Losier, P.; Rogers, R. D.; Zaworotko, M. J. *Angew. Chem., Int. Ed. Engl.* **1997**, *36*, 972−973.

(7) (a) Ma, S. H.; Rudkevich, D. M.; Rebek, J. *Angew. Chem., Int. Ed.* **1999**, *38*, 2600−2602. (b) Masaoka, S.; Tanaka, D.; Nakanishi, Y.; Kitagawa, S. *Angew. Chem., Int. Ed.* **2004**, *43*, 2530−2534. (c) Jones, C. D.; Tan, J. C.; Lloyd, G. O. *Chem. Commun.* **2012**, *48*, 2110−2112. (d) Zhang, J. P.; Huang, X. C.; Chen, X. M. *Chem. Soc. Rev.* **2009**, *38*, 2385−2396. (e) Abourahma, H.; Moulton, B.; Kravtsov, V.; Zaworotko, M. J. *J. Am. Chem. Soc.* **2002**, *124*, 9990−9991.

(8) Masaoka, S.; Tanaka, D.; Nakanishi, Y.; Kitagawa, S. *Angew. Chem., Int. Ed.* **2004**, *43*, 2530−2534.

(9) (a) Lee, I. S.; Shin, D. M.; Chung, Y. K. *Chem.—Eur. J.* **2004**, *10*, 3158−3165. (b) Huang, X. C.; Zhang, J. P.; Lin, Y. Y.; Chen, X. M. *Chem. Commun.* **2005**, 2232−2234. (c) Gale, P. A.; Light, M. E.; Quesada, R. *Chem. Commun.* **2005**, 5864−5866.

(10) Zhang, J. P.; Kitagawa, S. *J. Am. Chem. Soc.* **2008**, *130*, 907−917.

(11) (a) Park, I. H.; Lee, S. S.; Vittal, J. J. *Chem.—Eur. J.* **2013**, *19*, 2695−2702. (b) Aitipamula, S.; Nangia, A. *Chem.—Eur. J.* **2005**, *11*, 6727−6742.

(12) Li, S. L.; Tan, K.; Lan, Y. Q.; Qin, J. S.; Li, M. N.; Du, D. Y.; Zang, H. Y.; Su, Z. M. *Cryst. Growth. Des.* **2010**, *10*, 1699−1705.

(13) Hao, Z. M.; Zhang, X. M. *Cryst. Growth. Des.* **2007**, *7*, 64−68.

(14) Lee, E.; Kim, J. Y.; Lee, S. S.; Park, K. M. *Chem.—Eur. J.* **2013**, *19*, 13638−13645.

(15) (a) Lan, Y. Q.; Li, S. L.; Wang, X. L.; Shao, K. Z.; Su, Z. M.; Wang, E. B. *Inorg. Chem.* **2008**, *47*, 529−534. (b) Zhai, Q. G.; Wu, X. Y.; Chen, S. M.; Chen, L. J.; Lu, C. Z. *Inorg. Chim. Acta* **2007**, *360*, 3484−3492.

(16) Brown, I. D.; Altermatt, D. *Acta Crystallogr., Sect. B: Struct. Sci.* **1985**, *41*, 244−247.

(17) Antonio, M. R.; Soderholm, L. *Inorg. Chem.* **1994**, *33*, 5988−5993.

(18) Wang, X.-L.; Luan, J.; Lin, H.-Y.; Xu, C.; Liu, G.-C. *Inorg. Chim. Acta* **2013**, *408*, 139−144.

(19) Yang, C. Y.; Zhang, L. C.; Wang, Z. J.; Wang, L.; Li, X. H.; Zhu, Z. M. *J. Solid State Chem.* **2012**, *194*, 270−276.

(20) Martel, D.; Kuhn, A. *Electrochim. Acta* **2000**, *45*, 1829−1836.